

Rare charm meson decays $D \rightarrow Pl^+l^-$ and $c \rightarrow ul^+l^-$ in the standard model and the minimal supersymmetric standard model

S. Fajfer and S. Prelovsek

*Department of Physics, University of Ljubljana, Jadranska 19, 1000 Ljubljana, Slovenia
and J. Stefan Institute, Jamova 39, 1000 Ljubljana, Slovenia*

P. Singer

Department of Physics, Technion-Israel Institute of Technology, Haifa 32000, Israel

(Received 3 July 2001; published 7 November 2001)

We study the nine possible rare charm meson decays $D \rightarrow Pl^+l^-$ ($P = \pi, K, \eta, \eta'$) using heavy meson chiral Lagrangians and find them to be dominated by the long distance contributions. The decay $D^+ \rightarrow \pi^+ l^+ l^-$, with a branching ratio $\sim 1 \times 10^{-6}$, is expected to have the best chances for an early experimental discovery. The short distance contribution in the five Cabibbo suppressed channels arises via the $c \rightarrow ul^+l^-$ transition; we find that this contribution is detectable only in the $D \rightarrow \pi l^+ l^-$ decay, where it dominates the differential spectrum at high- q^2 . The general minimal supersymmetric standard model can enhance the $c \rightarrow ul^+l^-$ rate by up to an order of magnitude; its effect on the $D \rightarrow Pl^+l^-$ rates is small since the $c \rightarrow ul^+l^-$ enhancement is sizable in the low- q^2 region, which is inhibited in the hadronic decay.

DOI: 10.1103/PhysRevD.64.114009

PACS number(s): 13.25.Ft, 12.39.Fe, 12.39.Hg, 12.60.Jv

I. INTRODUCTION

The flavor-changing neutral processes are rare in the standard model (SM) and are of obvious interest in the search for new physics. Processes such as $c \rightarrow u\gamma$ and $c \rightarrow ul^+l^-$ are screened by the long distance contributions in the decays of charm hadrons [1,2], and one has to look for specific hadronic observables [3–5] in order to probe possible new physics [6,7]. The long distance contributions are also expected to dominate over the short distance contributions in $D^0-\bar{D}^0$ mixing [8], for which interesting experimental results have been reported recently [9].

The long and short distance contributions to rare charm meson decays $D \rightarrow Vl^+l^-$ with $V = \rho, \omega, \phi, K^*$ have been considered in Ref. [2]. The long distance contributions were shown to be largely dominant, and to screen possible effects of new physics in $c \rightarrow ul^+l^-$, unless these are very large. The experimental upper bounds on their branching ratios are presently in the 10^{-5} range [10], and are an order of magnitude larger than the standard model prediction for specific channels [2]. The decay $D_s^+ \rightarrow \rho^+ l^+ l^-$ is predicted at the highest rate $\sim 3 \times 10^{-5}$ [2], but there are unfortunately no experimental data on this particular channel.

In the present paper we consider the weak decays $D \rightarrow Pl^+l^-$ with pseudoscalar $P = \pi, K, \eta, \eta'$, some of which receive contributions from the $c \rightarrow ul^+l^-$ transition. These channels have not been observed so far, and only experimental upper bounds on the various branching ratios in the range $10^{-6}-10^{-4}$ exist [11–13]. The recent E791 analysis [11] considered all D^+ and D_s^+ decay channels. The most recent FOCUS analysis [12] provided upper bounds of about 8×10^{-6} on the $D^+ \rightarrow \pi^+ \mu^+ \mu^-$ and $D^+ \rightarrow K^+ \mu^+ \mu^-$ branching ratios, and is not far from our standard model prediction 1×10^{-6} for $D^+ \rightarrow \pi^+ \mu^+ \mu^-$. The limits on D^0 and D^+ modes at the level 10^{-6} are expected from CLEO-c and B

factories, while the limits on D_s^+ modes are expected to be an order of magnitude milder [14].

On the theoretical side, long distance contributions to $D \rightarrow \pi l^+ l^-$ decays have been considered in Ref. [15]. Here we also consider the long distance weak annihilation contribution and confirm it to be small in this channel. Calculations for other $D \rightarrow Pl^+l^-$ channels are not available in the literature. In the present work we investigate all these channels, including long-distance (LD) and possible short-distance (SD) contributions arising from the $c \rightarrow ul^+l^-$ transition. The QCD corrections to $c \rightarrow ul^+l^-$ amplitude have not yet been studied in detail and we incorporate only what we believe to be the most important QCD effects. We also explore the sensitivity of $c \rightarrow ul^+l^-$ transition to (i) minimal supersymmetric model with general soft-breaking terms, and (ii) two Higgs doublet model with flavor changing neutral Higgs interactions.

The $c \rightarrow ul^+l^-$ transition in SM, minimal supersymmetric standard model (MSSM), and two Higgs doublet model is studied in Sec. II. The long distance contributions are considered within the heavy meson chiral Lagrangian approach in Sec. III. Results are compiled in Sec. IV, while conclusions are given in Sec. V.

II. THE $c \rightarrow ul^+l^-$ DECAY

The Lagrangian leading to the $c \rightarrow ul^+l^-$ transition is (using notation as in Ref. [16])

$$\mathcal{L} = -\frac{4G_F}{\sqrt{2}} V_{cs}^* V_{us} \left[c_7 \mathcal{O}_7 + c_7' \mathcal{O}_7' + \frac{\alpha}{4\pi} \{ c_9 \mathcal{O}_9 + c_9' \mathcal{O}_9' + c_{10} \mathcal{O}_{10} + c_{10}' \mathcal{O}_{10}' \} \right], \quad (1)$$

where

$$\begin{aligned}\mathcal{O}_7 &= \frac{e}{16\pi^2} m_c \bar{u} \sigma^{\mu\nu} P_R c F_{\mu\nu}, & \mathcal{O}_9 &= \bar{u} \gamma^\mu P_L c \bar{l} \gamma_\mu l, \\ \mathcal{O}_{10} &= \bar{u} \gamma^\mu P_L c \bar{l} \gamma_\mu \gamma_5 l, & \mathcal{O}'_7 &= \frac{e}{16\pi^2} m_c \bar{u} \sigma^{\mu\nu} P_L c F_{\mu\nu}, \\ \mathcal{O}'_9 &= \bar{u} \gamma^\mu P_R c \bar{l} \gamma_\mu l, & \mathcal{O}'_{10} &= \bar{u} \gamma^\mu P_R c \bar{l} \gamma_\mu \gamma_5 l,\end{aligned}\quad (2)$$

with $P_{R,L} = (1 \pm \gamma_5)/2$. In Eq. (1) only the Cabibbo-Kobayashi-Maskawa (CKM) matrix element $V_{cs}^* V_{us}$ appears, for reasons explained in Sec. II A [18]. The Wilson coefficients in various scenarios are given in the following sections. The differential branching ratio is given by [16]

$$\begin{aligned}\frac{dBr(c \rightarrow ul^+ l^-)}{ds} &\equiv \frac{1}{\Gamma(D^0)} \frac{d\Gamma(c \rightarrow ul^+ l^-)}{ds} \\ &= \left[\frac{G_F^2 m_c^5}{192 \pi^3 \Gamma(D^0)} \right] \frac{\alpha^2}{4 \pi^2} |V_{cs}^* V_{us}|^2 (1-s)^2 \\ &\quad \times \{ [(1+2s)(|c_9|^2 + |c_{10}|^2) \\ &\quad + 4(1+2/s)|c_7|^2 + 12Re[c_7^* c_9] \\ &\quad + \{c_{7,9,10} \rightarrow c'_{7,9,10}\}], \end{aligned}\quad (3)$$

where $s = m_l^2/m_c^2$, $m_c \simeq 1.5$ GeV and the mass of $l = e, \mu$ is neglected. The short-distance part of the $D \rightarrow Pl^+ l^-$ amplitude, which is induced by $c \rightarrow ul^+ l^-$ transition, is given by Eq. (A2) in the Appendix.

A. Standard model

The $c \rightarrow ul^+ l^-$ amplitude is given by the γ and Z penguin diagrams and the W box diagram at one-loop electroweak order in the standard model, and is dominated by light quarks in the loop. One has [2,17]

$$\begin{aligned}c_9(m_W) &\simeq \frac{4}{9} \ln \frac{m_s}{m_d} = 1.34 \pm 0.09, \\ c_{7,10}(m_W) &\propto \frac{m_{d,s}^2}{m_W^2} \simeq 0, \\ c'_{7,9,10}(m_W) &\propto \frac{m_u}{m_c} c_{7,9,10} \simeq 0\end{aligned}\quad (4)$$

for $m_s/m_d = 21 \pm 4$ MeV [13], where the terms proportional to $m_{d,s}^2/m_W^2$ have been neglected. The leading term $\ln(m_s/m_d)$ in c_9 arises from the penguin diagram, with a photon emitted from the intermediate quark.

The QCD corrections to $c \rightarrow ul^+ l^-$ amplitude have not yet been studied in detail. The QCD corrections to c_7 , which are extremely small at the one-loop level, have been studied in Ref. [18] and are found to be large:

$$c_7^{eff}(m_c) = -(0.007 + 0.020i)[1 \pm 0.2]. \quad (5)$$

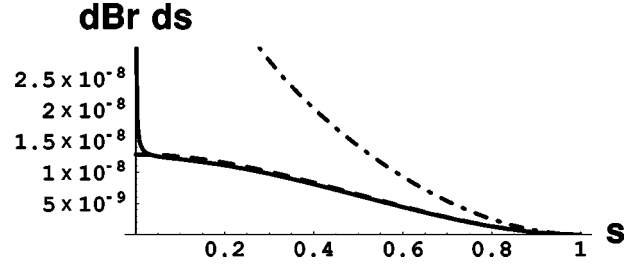


FIG. 1. The differential branching ratio $dBr(c \rightarrow ul^+ l^-)/ds$: the dashed line denotes the one-loop standard model prediction, while the solid line also incorporates the QCD corrections to c_7 [18]. The best enhancement of the $c \rightarrow ul^+ l^-$ rate in the general MSSM is given by the dot-dashed line, where the mass insertions are taken at their maximal values [Eqs. (9) and (10)], and $\alpha_s = 0.12$ and $M_{sq} = M_{gl} = 250$ GeV.

We expect the QCD corrections to c_9 to be rather unimportant, given that c_9 is already relatively large at the one-loop level [19]. We assume that the QCD corrections to c_{10} do not affect the $c \rightarrow ul^+ l^-$ rate significantly, and therefore use only the c_7 and c_9 coefficients. The differential branching ratios for cases with and without QCD corrections are shown by solid and dashed lines in Fig. 1, respectively. The branching ratio $[6 \pm 1] \times 10^{-9}$ is small, and arises mainly from c_9 ; the contribution from c_7 is small in spite of QCD enhancement.

B. Minimal supersymmetric standard model

New sources of flavor violation are present in the MSSM and these depend crucially on the mechanism of the supersymmetry breaking. The schemes with flavor-universal soft-breaking terms lead to contributions proportional to $\Sigma_{q=d,s,b} V_{cq}^* V_{uq} m_q^2$, and have negligible effects on the $c \rightarrow ul^+ l^-$ rate [20]. Our purpose here is to explore the largest possible enhancement of the $c \rightarrow ul^+ l^-$ rate in general MSSM with nonuniversal soft breaking terms. Based on the experience from the $c \rightarrow u \gamma$ decay [6,7], where the dominant contribution arises from gluino diagrams with the squark-mass insertion $(\delta_{12}^u)_{LR}$, we concentrate only on the gluino exchange diagrams with single mass insertion.¹ Following the analogous calculation for $b \rightarrow sl^+ l^-$ [16], we get for the Wilson coefficients in the MSSM

$$\begin{aligned}c_7^{gluino} &= \frac{e_u}{e_d} \frac{\sqrt{2}}{M_{sq}^2 G_F} \frac{1}{3} \frac{N_c^2 - 1}{2N_c} \frac{\pi \alpha_s}{V_{cs}^* V_{us}} \left[(\delta_{12}^u)_{LL} \frac{1}{4} P_{132}(z) \right. \\ &\quad \left. + (\delta_{12}^u)_{RL} P_{122}(z) \frac{M_{gl}}{m_c} \right] \leq 0.2,\end{aligned}\quad (6)$$

$$\begin{aligned}c_9^{gluino} &= -\frac{e_u}{e_d} \frac{\sqrt{2}}{M_{sq}^2 G_F} \frac{1}{3} \frac{N_c^2 - 1}{2N_c} \frac{\pi \alpha_s}{V_{cs}^* V_{us}} \frac{1}{3} P_{042}(z) (\delta_{12}^u)_{LL} \\ &\leq 0.002,\end{aligned}\quad (7)$$

¹We work in the super-CKM basis for squarks, where the squark-quark-gaugino vertex has the same flavor structure as the squark-quark-gauge boson vertex; for a review, see Ref. [21].

TABLE I. The second column represents the standard model prediction for $c \rightarrow ul^+l^-$ branching ratios, which is practically unaffected by the QCD corrections (see the text). The third column represents the biggest possible enhancement of the branching ratio in MSSM, evaluated for mass insertions at their maximal values [Eqs. (9) and (10)].

	Br^{SM}	Br^{MSSM} best enhanc.
$c \rightarrow ue^+e^-$	$(6 \pm 1) \times 10^{-9}$	6×10^{-8}
$c \rightarrow u\mu^+\mu^-$	$(6 \pm 1) \times 10^{-9}$	2×10^{-8}

$$c_{10}^{gluino} \simeq 0, \quad (8)$$

with $\alpha_s = \alpha_s(m_W) = 0.12$, $N_c = 3$, $z = M_{gl}^2/M_{sq}^2$, $P_{ijk}(z) = \int_0^1 dx \int_0^1 dy y^i (1-y)^j [1-y+zx y + z(1-x)y]^{-k}$, $e_u = 2/3$, and $e_d = -1/3$. The numerical bounds in Eqs. (6) and (7) are obtained by using parameter values discussed below. The expressions for $c'_{7,9,10}$ are obtained by replacing $L \leftrightarrow R$ in the formulas above. We use gluino mass $M_{gl} = 250$ GeV and a common value for squark masses of $M_{sq} = 250$ GeV, given by the lower experimental bounds [13].

The mass insertions are free parameters in a general MSSM. The strongest upper bound on $(\delta_{12}^u)_{LR}$ is obtained by requiring that the minima of the scalar potential do not break charge or color, and that they are bounded from below [22,6], giving

$$|\delta_{12}^u|_{LR}, |\delta_{12}^u|_{RL} \leq 0.0046 \quad \text{for } M_{sq} = 250 \text{ GeV}. \quad (9)$$

The insertions $(\delta_{12}^u)_{LL}$ and $(\delta_{12}^u)_{RR}$ can be bounded by saturating the experimental upper bound $\Delta m_D < 4.5 \times 10^{-14}$ GeV [9] by the gluino exchange [6,23]; the corresponding constraint on $(\delta_{12}^u)_{LR}$ is weaker than Eq. (9). Since we are interested in exhibiting the largest possible enhancement of the $c \rightarrow ul^+l^-$ rate, we saturate Δm_D by $(\delta_{12}^u)_{LL}$, obtaining [6,23]

$$|\delta_{12}^u|_{LL} \leq 0.03 \quad \text{for } M_{sq} = M_{gl} = 250 \text{ GeV}, \quad (10)$$

and we set $(\delta_{12}^u)_{RR} = 0$.

The largest possible enhancement of the $c \rightarrow ul^+l^-$ rate is obtained using the mass insertions at their upper bounds, and is shown by the dot-dashed line in Fig. 1. The effect is dominated by the gluino exchange diagrams induced by $(\delta_{12}^u)_{LR}$, and can enhance the $c \rightarrow ul^+l^-$ rate by nearly an order of magnitude, with the best enhancement displayed in Table I.

The supersymmetric enhancement of $c \rightarrow ul^+l^-$ is due to the increase in c_7 [Eq. (6)], and is manifested at small m_H due to the exchange of an almost real photon. This enhancing mechanism is unfortunately not present in $D \rightarrow Pl^+l^-$ decays [see Eq. (A2)] since the decay $D \rightarrow P\gamma$ with the real photon in the final state is forbidden [see Eq. (13)].

C. Flavor changing neutral Higgs boson

The tree-level exchange of a flavor changing neutral Higgs boson [24] turns out to have a negligible effect on the

$c \rightarrow ul^+l^-$ rate, due to the strong constraint coming from the experimental upper bound on Δm_D and due to the small masses of the leptons e and μ . Assuming the same $c-u-H$ coupling² f_{cu} and mass $m_H = 300$ GeV for all three neutral physical Higgs bosons in the two Higgs doublet model, and saturating the experimental upper bound $\Delta m_D \leq 4.5 \times 10^{-14}$ GeV [9],³

$$\frac{4}{3} \frac{f_{cu}^2}{m_H^2} f_D^2 m_D \leq (\Delta m_D)_{\text{expt}}, \quad (11)$$

we obtain $f_{cu} \leq 2 \times 10^{-4}$. This leads to a branching ratio

$$\text{Br}(c \rightarrow u\mu^+\mu^-)^{H^0} = \frac{5m_c^5}{768\pi^3\Gamma(D^0)} \left(\frac{f_{cu}m_\mu}{vm_H^2} \right)^2 \leq 7 \times 10^{-16}. \quad (12)$$

Thus, unlike the supersymmetric model, the experimental upper bound on Δm_D makes this new contribution negligible.

The authors of Ref. [25] studied the constraints on the parameters of this model imposed by the present data on the semileptonic and leptonic D decays. Since they did not consider the constraint coming from the $D^0 - \bar{D}^0$ mixing, they obtained rather mild constraints.

III. LONG DISTANCE CONTRIBUTIONS

Now we turn to an estimate of the long distance contributions to the $D \rightarrow Pl^+l^-$ decays. The dominant long distance contributions arise via the weak transition $D \rightarrow P\gamma^*$, followed by $\gamma^* \rightarrow l^+l^-$. The general Lorentz structure of the $D \rightarrow P\gamma^*$ amplitude, consistent with electromagnetic gauge invariance, is [26]

$$\mathcal{A}[D(p) \rightarrow P(p')\gamma^*(q, \epsilon)] \propto A(q^2) \epsilon_\mu^* [q^2(p+p')^\mu - (m_D^2 - m_P^2)q^\mu], \quad (13)$$

and this amplitude vanishes for the case of a real photon. The factor q^2 in Eq. (13) cancels the photon propagator $1/q^2$, and the general amplitude has the form

$$\begin{aligned} \mathcal{A}[D(p) \rightarrow P\gamma^* \rightarrow Pl^+(p_+)l^-(p_-)] \\ = i \frac{G_F}{\sqrt{2}} e^2 A(q^2) \bar{u}(p_-) \not{p} v(p_+). \end{aligned} \quad (14)$$

The long distance contribution is induced by the effective nonleptonic weak Lagrangian

²The coupling is f_{cu} for $c-u-H_{1,2}^0$ and $f_{cu}\gamma_5$ for $c-u-A^0$.

³The matrix elements of four-fermion operators are evaluated according to Ref. [23].

$$\mathcal{L}^{|\Delta c|=1} = -\frac{G_F}{\sqrt{2}} V_{cq_j}^* V_{uq_i} [a_1 \bar{u} \gamma^\mu (1 - \gamma_5) q_i \bar{q}_j \gamma_\mu (1 - \gamma_5) c + a_2 \bar{q}_j \gamma_\mu (1 - \gamma_5) q_i \bar{u} \gamma^\mu (1 - \gamma_5) c], \quad (15)$$

accompanied by the emission of the virtual photon. Here $q_{i,j}$ denote the d or s quark fields. The coefficients $a_1 = 1.2$ and $a_2 = -0.5$ have been determined from the experimental data on nonleptonic charm meson decays in an extensive analysis based on the factorization approximation of Ref. [27]. We also systematically undertake a factorization approximation to evaluate the matrix element for the product of the currents [Eq. (15)].

In order to treat the transition among physical particles, we shall use an effective Lagrangian approach with a heavy pseudoscalar D , a heavy vector D^* , and a light pseudoscalar P , and also including light vector V degrees of freedom. The latter are necessary since they play a dynamical role in the photon emission from a meson via vector meson dominance (VMD) and lead to the resonant spectrum in terms of invariant dilepton mass m_{ll} . We organize various effective interactions among the mesonic degrees of freedom following the heavy meson chiral Lagrangian approach [28], which was reviewed in Ref. [29] and is most likely the best suited framework for treating the problem under investigation. It embodies two important global symmetries of QCD: the heavy quark spin and flavor symmetry $SU(2N_f)$ in the limit $m_c \rightarrow \infty$ and chiral symmetry $SU(3)_L \times SU(3)_R$, spontaneously broken to $SU(3)_V$, in the limit $m_{u,d,s} \rightarrow 0$. The light vector mesons are introduced by promoting the symmetry $G = [SU(3)_L \times SU(3)_R]_{global} / [SU(3)_V]_{global}$ to $G' = [SU(3)_L \times SU(3)_R]_{global} \times [SU(3)_V]_{local}$, where the light

vector resonances are identified with the gauge bosons of $[SU(3)_V]_{local}$ [30]. One is free to fix the gauge of $[SU(3)_V]_{local}$ and the two theories, based on the groups G and G' , are equivalent up to terms with derivatives on the light vector fields [30].

Keeping only the kinetic and interaction terms of the lowest nontrivial order, the Lagrangian has the form [29,32]

$$\begin{aligned} \mathcal{L} = & -\frac{f^2}{2} \{ \text{tr}[\mathcal{A}_\mu \mathcal{A}^\mu] + a \text{tr}[(\mathcal{V}_\mu - \rho_\mu)^2] \\ & + \frac{1}{2g_V^2} \text{tr}[F_{\mu\nu}(\rho) F^{\mu\nu}(\rho)] \\ & + i \text{Tr} \left[H_b v_\mu \left\{ \delta_{ba} \partial^\mu - i \frac{2}{3} e \delta_{ba} A^\mu + \mathcal{V}_{ba}^\mu \right. \right. \\ & \left. \left. - \kappa (\mathcal{V}^\mu - \rho^\mu)_{ba} \right\} \bar{H}_a \right] + i g \text{Tr}[H_b \gamma_\mu \gamma_5 A_{ba}^\mu \bar{H}_a], \end{aligned} \quad (16)$$

with

$$\mathcal{A}_\mu = \frac{1}{2} [\xi^\dagger (\partial_\mu + ieQA_\mu) \xi - \xi (\partial_\mu + ieQA_\mu) \xi^\dagger],$$

$$\mathcal{V}_\mu = \frac{1}{2} [\xi^\dagger (\partial_\mu + ieQA_\mu) \xi + \xi (\partial_\mu + ieQA_\mu) \xi^\dagger],$$

$Q = \text{diag}(2/3, -1/3, -1/3)$ and photon field A_μ . The light fields are incorporated in

$$\xi = \exp \frac{i}{f} \begin{pmatrix} \frac{\pi^0}{\sqrt{2}} + \left[\frac{\eta_8}{\sqrt{6}} + \frac{\eta_0}{\sqrt{3}} \right] & & \pi^+ & & K^+ \\ & \pi^- & -\frac{\pi^0}{\sqrt{2}} + \left[\frac{\eta_8}{\sqrt{6}} + \frac{\eta_0}{\sqrt{3}} \right] & & K^0 \\ & & & \bar{K}^0 & \\ & K^- & & & \left[-\frac{2\eta_8}{\sqrt{6}} + \frac{\eta_0}{\sqrt{3}} \right] \end{pmatrix}, \quad (17)$$

$$\rho_\mu = i \frac{\tilde{g}_V}{\sqrt{2}} \begin{pmatrix} \frac{\rho_\mu^0 + \omega_\mu}{\sqrt{2}} & \rho_\mu^+ & K_\mu^{*+} \\ \rho_\mu^- & -\frac{\rho_\mu^0 + \omega_\mu}{\sqrt{2}} & K_\mu^{*0} \\ K_\mu^{*-} & \bar{K}_\mu^{*0} & \phi_\mu \end{pmatrix},$$

TABLE II. The branching ratios for nine $D \rightarrow Pl^+l^-$ decays in the standard model. The short distance contributions, induced by the $c \rightarrow ul^+l^-$ transition, are given in column 2 and are small. The total branching ratio is therefore dominated by the long distance contribution, and is given in column 3. The experimental upper bounds are given in the last two columns [13,11,12]: the E791 analysis [11] considers D^+ and D_s^+ decays, while the new analysis of FOCUS [12] considers only D^+ decays. The MSSM has insignificant effect on the total rates of $D \rightarrow Pl^+l^-$ decays.

$D \rightarrow Pl^+l^-$	Br_{SM}^{SD} $l = \mu, e$	$\text{Br}_{SM} \simeq \text{Br}^{LD}$ $l = \mu, e$	Br^{expt} $l = e$	Br^{expt} $l = \mu$
$D^0 \rightarrow \bar{K}^0 l^+ l^-$	0	4.3×10^{-7}	$< 1.1 \times 10^{-4}$	$< 2.6 \times 10^{-4}$
$D_s^+ \rightarrow \pi^+ l^+ l^-$	0	6.1×10^{-6}	$< 2.7 \times 10^{-4}$	$< 1.4 \times 10^{-4}$
$D^0 \rightarrow \pi^0 l^+ l^-$	1.9×10^{-9}	2.1×10^{-7}	$< 4.5 \times 10^{-5}$	$< 1.8 \times 10^{-4}$
$D^0 \rightarrow \eta l^+ l^-$	2.5×10^{-10}	4.9×10^{-8}	$< 1.1 \times 10^{-4}$	$< 5.3 \times 10^{-4}$
$D^0 \rightarrow \eta' l^+ l^-$	9.7×10^{-12}	2.4×10^{-10}	$< 1.1 \times 10^{-4}$	$< 5.3 \times 10^{-4}$
$D^+ \rightarrow \pi^+ l^+ l^-$	9.4×10^{-9}	1.0×10^{-6}	$< 5.2 \times 10^{-5}$	$< 7.8 \times 10^{-6}$
$D_s^+ \rightarrow K^+ l^+ l^-$	9.0×10^{-10}	4.3×10^{-8}	$< 1.6 \times 10^{-3}$	$< 1.4 \times 10^{-4}$
$D^+ \rightarrow K^+ l^+ l^-$	0	7.1×10^{-9}	$< 2.0 \times 10^{-4}$	$< 8.1 \times 10^{-6}$
$D^0 \rightarrow K^0 l^+ l^-$	0	1.1×10^{-9}		

where η_8 and η_0 contribute to $\eta - \eta'$ mixing as in Ref. [13] with $\theta_p = -20 \pm 5^\circ$. The heavy pseudoscalar D_a and vector D_a^* fields of flavor $c\bar{q}_a$ are incorporated in

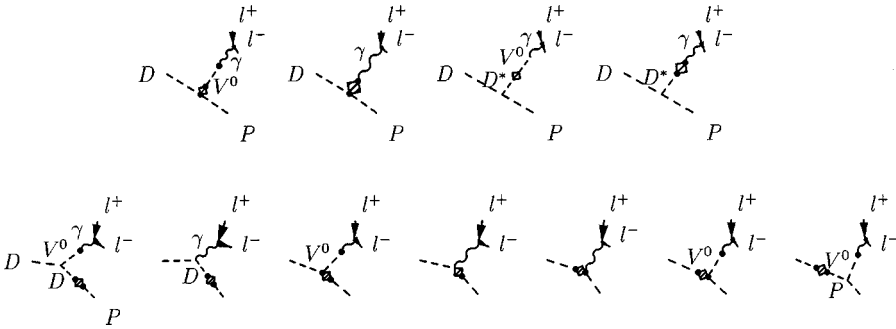
$$H_a = \frac{1}{2}(1 + \not{\theta})[-D_a^v \gamma_5 + D_{a\mu}^{*v} \gamma^\mu],$$

$$\bar{H}_a = \gamma^0 H_a \gamma^0. \quad (18)$$

Above, $f = 132$ MeV is the pseudoscalar decay constant and $\tilde{g}_V = 5.8$ is the VPP coupling [29,30]. We fix $a = 2$ assuming the exact vector meson dominance, when the light pseudoscalars interact with the photon only through the vector mesons [29,30,32]. We shall use $g = 0.59 \pm 0.06$, obtained by CLEO from the measurement of the widths $D^{*+} \rightarrow D^0 \pi^+$ and $D^{*+} \rightarrow D^+ \pi^0$ [33]. The parameter κ will eventually turn out to be multiplied by a small factor m_P^2 in the $D \rightarrow Pl^+l^-$ amplitudes and its contribution is negligible.

The bosonized weak current coming from the light quarks is obtained by gauging Eq. (16):

$$\bar{q}_a \gamma^\mu (1 - \gamma_5) q_b \simeq (if^2 \xi [\mathcal{A}^\mu + a(\mathcal{V} - \rho)^\mu] \xi^\dagger)_{ba}. \quad (19)$$



The weak current $\bar{q}_a \gamma^\mu (1 - \gamma_5) c$ transforms under chiral $SU(3)_L \times SU(3)_R$ transformation as $(\bar{3}_L, 1_R)$, and is linear in the heavy meson fields D^a and D_μ^{*a} [31,32]:

$$\begin{aligned} \bar{q}_a \gamma^\mu (1 - \gamma_5) c \simeq & \frac{1}{2} i f_D \sqrt{m_D} \text{Tr}[\gamma^\mu (1 - \gamma_5) H_b \xi_{ba}^\dagger] \\ & + \alpha_1 \text{Tr}[\gamma_5 H_b (\rho^\mu - \mathcal{V}^\mu)_{bc} \xi_{ca}^\dagger] \\ & + \alpha_2 \text{Tr}[\gamma^\mu \gamma_5 H_b \mathcal{V}_a (\rho^\alpha - \mathcal{V}^\alpha)_{bc} \xi_{ca}^\dagger] + \dots \end{aligned} \quad (20)$$

This current is the most general one at the leading order in the heavy quark and next-to-leading order in the chiral expansion. The parameters α_1 and α_2 are determined from experimental data on Br , Γ_L/Γ_T and Γ_+/ Γ_- of the decay $D^+ \rightarrow \bar{K}^{*0} e^+ \nu_e$ [13]. Among the eight sets of solutions for three parameters [31], we use the set $\alpha_1 = 0.14 \pm 0.01$ $\text{GeV}^{1/2}$ and $\alpha_2 = 0.10 \pm 0.03$ $\text{GeV}^{1/2}$ which agrees with the measured form factors.

We shall calculate a larger group of $D \rightarrow Pl^+l^-$ decays, rather than only those related to $c \rightarrow ul^+l^-$ transition. The list of decays considered is given in Table II. The Feynman diagrams for the long distance contributions to $D \rightarrow Pl^+l^-$

FIG. 2. Long distance contributions to $D \rightarrow Pl^+l^-$ decays. The vector meson V^0 denotes ρ^0 , ω , or ϕ . The box denotes the action of the nonleptonic effective Lagrangian [Eq. (15)]. The box contains two dots each denoting a weak current in the Lagrangian [Eq. (15)].

TABLE III. The values of the meson masses, decay constants, and decay widths [13]. The measured decay constants f_D and f_{D^*} have sizable uncertainties, and the values are taken from lattice QCD results [38].

H	m_H (GeV)	f_H (GeV)	P	m_P (GeV)	f_P (GeV)
D	1.87	0.21	π	0.14	0.135
D_s	1.97	0.24	K	0.50	0.16
D^*	2.01	0.21	η	0.55	0.13
			η'	0.96	0.11

within our framework are given in Fig. 2. The Lagrangian (15) contains a product of two left handed quark currents, each denoted by a dot in a box. We organize different diagrams according to the factorization of the nonleptonic effective Lagrangian (15).

The long distance penguin contribution [34] in Fig. 2(a) is induced by $[\bar{s}\gamma_\mu s - \bar{d}\gamma_\mu d]u\gamma^\mu(1 - \gamma_5)c$.

The long distance weak annihilation in Fig. 2(b) is induced by a product of the weak currents, where one current has the flavor of the initial D meson, while the other has the flavor of the final P meson. Vector resonances do not enter as intermediate states R in the weak transition $D \rightarrow R$ followed by $R \rightarrow P\gamma^*$ or $D \rightarrow R\gamma^*$ followed by the weak transition $R \rightarrow P$, since parity is conserved in $D \rightarrow P\gamma^*$ process.

The Lagrangian (16) and the weak currents [Eqs. (19) and (20)] are invariant under the electromagnetic gauge transformation, and automatically lead to the gauge invariant amplitude of the form of Eq. (13). This is due to the fact that the vector field ρ_μ and the vector current $\mathcal{V}_\mu = ieQA_\mu + \frac{1}{2}(\xi^\dagger \partial_\mu \xi + \xi \partial_\mu \xi^\dagger)$ always appear in the gauge invariant combination $\mathcal{V}_\mu - \rho_\mu$ and the resonant and nonresonant diagrams in Fig. 2 come in pairs.

We incorporate SU(3) symmetry breaking by using the physical masses, widths and decay constants, given in Tables III and IV of the Appendix with the definition

$$\begin{aligned} \langle 0|j^\mu|P\rangle &= if_P p^\mu, & \langle 0|j^\mu|D\rangle &= -if_D p^\mu, \\ \langle 0|j^\mu|V\rangle &= g_V \epsilon^\mu, & \langle 0|j^\mu|D^*\rangle &= if_{D^*} m_{D^*} \epsilon^\mu \end{aligned} \quad (21)$$

and properly normalized for $j^\mu = \bar{q}_1 \gamma^\mu (1 - \gamma_5) q_2$. The assumptions for extrapolating the amplitudes away from where the chiral and heavy quark symmetries are good are discussed in the Appendix. The amplitudes for the diagrams in Fig. 2 are given by Eq. (A5).

IV. RESULTS

The allowed kinematical region for the dilepton mass m_{ll} in the $D \rightarrow Pl^{+}l^{-}$ decay is $m_{ll} = [2m_l, m_D - m_P]$. The long distance contribution has a resonant shape with poles at $m_{ll} = m_{\rho^0}, m_\omega, m_\phi$. There is no pole at $m_{ll} = 0$ since the decay $D \rightarrow P\gamma$ is forbidden. The short distance contribution is rather flat. The spectra of $D \rightarrow Pe^+e^-$ and $D \rightarrow P\mu^+\mu^-$ decays in terms of m_{ll} are practically identical. The difference in their rates due to the kinematical region m_{ll}

TABLE IV. The masses, widths, and decay constants of ground [13] and excited [35,36] vector mesons.

	ρ	ω	ϕ	ρ_1	ω_1	ϕ_1	ρ_2	ω_2	ϕ_2
m (GeV)	0.77	0.78	1.0	1.45	1.46	1.69	1.66	1.66	1.88
Γ (GeV)	0.15	0.0084	0.0044	0.31	0.24	0.3	0.4	0.1	0.3
g_V (GeV ²)	0.17	0.15	0.24	0.11	0.11	0.23	0.07	0.07	0.12

$= [2m_e, 2m_\mu]$ is small, and we do not consider them separately. The predicted branching ratios for nine decays in the standard model are given in Table II together with the available experimental data [11–13]. The short distance contribution, as predicted by the standard model, is given in the second column and is small. The total branching ratio is therefore dominated by the long distance contribution and is given in column 3.

The differential branching ratio dBr/dm_{ll}^2 for the Cabibbo allowed decay $D_s^+ \rightarrow \pi^+ l^+ l^-$, which arises only via the weak annihilation, is presented in Fig. 3(a). In Fig. 3(b), we present the Cabibbo suppressed decay $D \rightarrow \pi l^+ l^-$, in which the kinematical upper bound on the dilepton mass $m_{ll}^{max} = m_D - m_P$ is the highest. The dashed and dot-dashed lines denote the long and short distance parts of the rate in the SM, respectively, while the solid lines denote the total rate. The long distance contribution decreases in the kinematical region above the resonance ϕ and the short distance contribution becomes dominant. Thus the decays $D^{+,0} \rightarrow \pi^{+,0} l^+ l^-$ at high m_{ll} might present a unique opportunity to probe the flavor changing neutral transition $c \rightarrow ul^+ l^-$ in the future. As the pion is the lightest hadron state, this interesting kinematical region is not present in other $D \rightarrow Xl^+ l^-$ decays.

The differential distribution for $D^+ \rightarrow \pi^+ l^+ l^-$, given in Fig. 3, indicates that the high dilepton mass region might give an opportunity for detecting $c \rightarrow ul^+ l^-$. Before making a definite statement on such a possibility, we should examine this kinematical region of high dilepton mass in $D \rightarrow \pi l^+ l^-$ decays more closely. For instance, in this region the excited states of the vector mesons ρ , ω , and ϕ may become important. We attempt a rough estimate of the additional long distance contribution arising from the first radial excited states ρ_1 , ω_1 , and ϕ_1 (3S_1) and first orbital excited states ρ_2 , ω_2 , and ϕ_2 (3D_1). The knowledge of their masses, decay widths, and couplings to other particles is poor at present. We use the measured masses and widths, taken from Refs. [13,35] and compiled in Table IV. Due to the lack of experimental data on the leptonic decay widths [35], we use the magnitudes of the decay constants g_V as predicted by the quark model in Ref. [36]⁴ and compiled in Table IV. At the same time, we assume that the excited vector mesons couple to the charmed mesons with the same couplings as the corresponding ground state vector mesons ρ , ω , and ϕ . In this case, the corresponding amplitudes [Eqs. (A5)] are obtained

⁴The decay constant f_V , defined in Ref. [36], is related to g_V , defined in Eq. (21), by: $f_\rho \rightarrow \sqrt{2}m_\rho f_\rho$, $f_\omega \rightarrow 3\sqrt{2}m_\omega f_\omega$, and $f_\phi \rightarrow -3m_\phi f_\phi$.

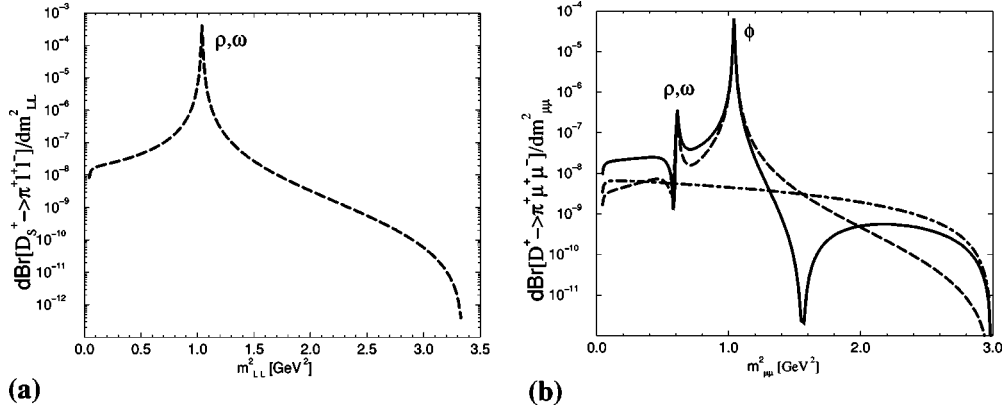


FIG. 3. The differential branching ratios dBr/dm_{ll}^2 as a function of the invariant dilepton mass m_{ll}^2 for the Cabibbo allowed decay $D_s^+ \rightarrow \pi^+ l^+ l^-$ (a) and Cabibbo suppressed decay $D^+ \rightarrow \pi^+ l^+ l^-$ (b). The dashed line denotes the long distance contribution, the dot-dashed line denotes the $c \rightarrow ul^+l^-$ induced short distance contribution, and the solid line denotes the total standard model prediction. The $D_s^+ \rightarrow \pi^+ l^+ l^-$ arises only via the long distance contribution.

by replacing the coefficients N_1 and M_1 by the expressions given in Eq. (A7). The differential branching ratios for $D \rightarrow \pi \mu^+ \mu^-$ decays are given in Fig. 4. The thick and thin dashed lines denote the long distance contributions with and without excited vector mesons, respectively. The short distance contribution, denoted by the dot-dashed line, is still dominant in the kinematical region of high m_{ll} in spite of the excited vector resonances.

The possible enhancement within the general MSSM, discussed in Sec. II, is presented in Fig. 5 and is probably too small to be observed in any $D \rightarrow Pl^+l^-$ decay. The solid lines represent the standard model prediction for the $D \rightarrow \pi l^+ l^-$ branching ratios. The dot-dashed lines represent the best enhancement in the general MSSM, and indicate that the $D \rightarrow Pl^+l^-$ rates are rather insensitive to the large supersymmetric enhancement of c_7 . The value of c_7 is manifested in $c \rightarrow ul^+l^-$ at small m_{ll} [see Eq. (3) and Fig. 1], while its effect is suppressed in $D \rightarrow Pl^+l^-$ decays due to the factor q^2 in the general expression for the $D \rightarrow P\gamma^*$ amplitude [Eq. (13)].

V. CONCLUSIONS

We have presented the first predictions for rare charm meson decays $D \rightarrow Pl^+l^-$ with $P = \pi, K, \eta, \eta'$ in all nine possible channels; a previous analysis [15] has considered only the $D \rightarrow \pi l^+ l^-$ channel. The long distance contributions are found to dominate over the short distance contributions, which are induced by $c \rightarrow ul^+l^-$ in the Cabibbo-suppressed decays. We have used the theoretical framework of heavy meson chiral Lagrangian with the recently determined value of the strong coupling g from the measurement of $D^* \rightarrow D\pi$ width. Our predictions are compiled in Table II. The decay $D_s^+ \rightarrow \pi^+ l^+ l^-$ is predicted at the highest branching ratio of 6×10^{-6} . The best chances of the experimental discovery are expected for $D^+ \rightarrow \pi^+ l^+ l^-$, which is predicted at 1×10^{-6} and has the upper bound 8×10^{-6} [12] at present. The limits on D^0 and D^+ modes at the level 10^{-6} are expected from CLEO-c and B factories, while the limits on D_s^+ modes are expected to be an order of magnitude milder [14]. The only possibility to look for $c \rightarrow ul^+l^-$ transition is represented by $D \rightarrow \pi l^+ l^-$ decays in the kinematical region

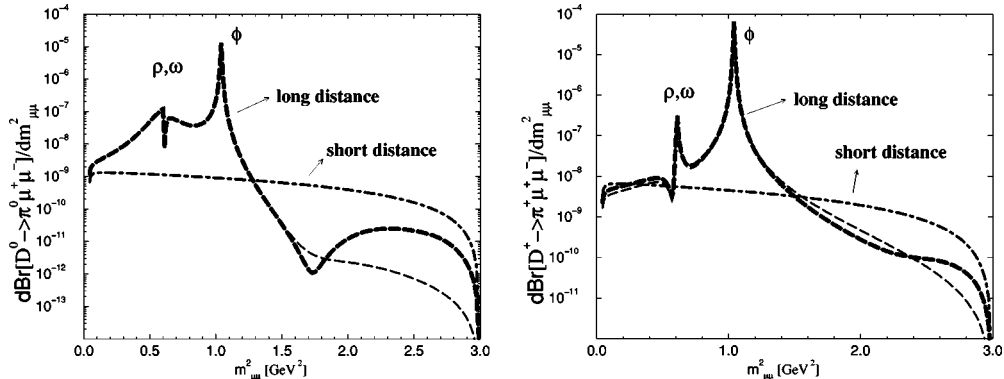


FIG. 4. The differential branching ratio for $D \rightarrow \pi \mu^+ \mu^-$ decays. The thick dashed lines present the long distance contribution incorporating the ground state and the excited vector mesons. The thin dashed lines present the long distance contributions due only to the ground vector mesons. The short distance contribution, denoted by the dot-dashed line, is dominant in the kinematical region of high m_{ll} , in spite of the excited vector resonances.

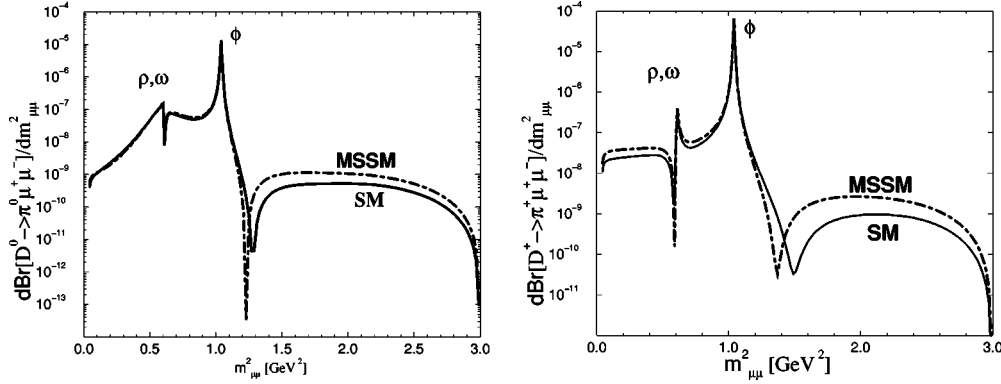


FIG. 5. The largest possible enhancement of $D \rightarrow \pi \mu^+ \mu^-$ rates within the general MSSM, discussed in Sec. II A, is denoted by the dot-dashed lines. The solid lines represent the standard model predictions. The effect of supersymmetry is screened by the uncertainties present in the determination of the long distance contributions, and is probably too small to be observed.

of m_{H} above the resonance ϕ , where the long distance contribution is reduced (see Fig. 4).

We have explored the sensitivity of the $c \rightarrow u l^+ l^-$ within two scenarios of physics beyond the SM. The effect due to the exchange of the flavor changing Higgs boson in the two Higgs doublet model is found to be negligible. The general minimal supersymmetric standard model can enhance the $c \rightarrow u \mu^+ \mu^-$ rate by up to a factor of three (see Table I). This effect is due to the large supersymmetric enhancement of c_7 and is sizable at small m_{H} in $c \rightarrow u l^+ l^-$, but it is unfortunately very small in the hadronic process $D \rightarrow P l^+ l^-$ as the decay $D \rightarrow P \gamma$ is forbidden (see Fig. 5).

The kinematics of the processes $D \rightarrow V l^+ l^-$ would be more favorable to probe the possible supersymmetric enhancement at small m_{H} , but the long distance contributions in these channels are even more disturbing [2]. The large supersymmetric enhancement of the Wilson coefficient c_7 is manifested in $c \rightarrow u \gamma$ decay, and can enhance the standard model rate $\sim 10^{-8}$ by up to two orders of magnitude [6,7]. Such an enhancement could be probed by observation of $B_c \rightarrow B_u^* \gamma$ [3] or by measuring the relative difference $\text{Br}(D^0 \rightarrow \rho^0 \gamma) - \text{Br}(D^0 \rightarrow \omega \gamma)$ [4].

APPENDIX

The short distance part of the $D \rightarrow P l^+ l^-$ amplitude, induced by the transition $c \rightarrow u l^+ l^-$, contains the form factors

$$\begin{aligned}
 \langle P(p') | \bar{q} \gamma_\mu (1 - \gamma_5) c | D(p) \rangle &= (p + p')_\mu f_+(q^2) \\
 &\quad + (p - p')_\mu f_-(q^2), \\
 \langle P(p') | \bar{q} \sigma_{\mu\nu} (1 \pm \gamma_5) c | D(p) \rangle &= i s(q^2) [(p + p')_\mu q_\nu \\
 &\quad - q_\mu (p + p')_\nu \\
 &\quad \pm i \epsilon_{\mu\nu\lambda\sigma} (p + p')^\lambda q^\sigma]
 \end{aligned} \tag{A1}$$

defined using operators in Eq. (1). The short distance amplitude is then given by

$$\begin{aligned}
 \mathcal{A}^{SD}[D(p) \rightarrow P(p-q) l^+ l^-] \\
 &= i \frac{G_F}{\sqrt{2}} e^2 V_{cs}^* V_{us} \left[-\frac{c_7 + c_7'}{2\pi^2} m_c s(q^2) \right. \\
 &\quad \left. - \frac{c_9}{4\pi^2} f_+(q^2) \right] \bar{u}(p_-) \not{p} v(p_+), \tag{A2}
 \end{aligned}$$

where we neglected the nearly vanishing c_{10} , c_9' and c_{10}' coefficients in SM [Eq. (4)] and MSSM [Eq. (8)]. In the heavy quark limit, the form factor s can be expressed in terms of the form factors f_\pm at zero recoil [39],⁵ and we assume the relation to be valid for all q^2 :

$$s(q^2) = \frac{1}{2m_D} [f_+(q^2) - f_-(q^2)]. \tag{A3}$$

The semileptonic form factors f_\pm in the heavy meson chiral Lagrangian approach, extended by assuming a polar shape, are given by [28,29]⁶

$$\begin{aligned}
 f_+(q^2) &= -f_-(q^2) \\
 &= -K_{DP} \frac{f_D}{2} \left[g \frac{m_D - m_P}{m_P + m_{D'^*} - m_D} \right] \frac{m_{D'^*}^2 - q_{max}^2}{m_{D'^*}^2 - q^2},
 \end{aligned} \tag{A4}$$

with K_{DP} given in Table V.

The long distance amplitude is given by the diagrams in Fig. 2. The long distance penguin diagrams in Fig. 2(a) are expressed in terms of the form factor f_+ [Eq. (A4)]. The

⁵This relation was not written correctly in Ref. [39], and was corrected in Ref. [29].

⁶Different form factors f_\pm were used together with $g \approx 0.27$ in Ref. [32]. These form factors would overproduce the semileptonic decay rates for the value $g \approx 0.59$ recently measured by CLEO [33].

TABLE V. The Cabibbo factors $f_{Cabb}^{(i)}$, the coefficients $K_{DP}^{(i)}$ and the functions $M_1^{(i)}$ for nine $D \rightarrow Pl^+l^-$ amplitudes in Eq. (A5).

i	$D \rightarrow Pl^+l^-$	$f_{Cabb}^{(i)}$	$M^{(i)}$	$K_{DP}^{(i)}$
1	$D^0 \rightarrow \bar{K}^0 l^+ l^-$	$a_2 V_{ud} V_{cs}^*$	$M_1^{D^0}$	0
2	$D_s^+ \rightarrow \pi^+ l^+ l^-$	$a_1 V_{ud} V_{cs}^*$	$M_1^{D_s^+}$	0
3	$D^0 \rightarrow \pi^0 l^+ l^-$	$-a_2 V_{ud} V_{cd}^*$	$-\frac{1}{\sqrt{2}} M_1^{D^0}$	$\frac{1}{\sqrt{2} f_\pi}$
4	$D^0 \rightarrow \eta l^+ l^-$	$a_2 V_{ud} V_{cd}^*$	$-\sqrt{\frac{3}{2}} M_1^{D^0} \cos \theta_P$	$\frac{\cos \theta_P}{\sqrt{6} f} - \frac{\sin \theta_P}{\sqrt{3} f}$
5	$D^0 \rightarrow \eta' l^+ l^-$	$a_2 V_{ud} V_{cd}^*$	$-\sqrt{\frac{3}{2}} M_1^{D^0} \sin \theta_P$	$\frac{\sin \theta_P}{\sqrt{6} f} + \frac{\cos \theta_P}{\sqrt{3} f}$
6	$D^+ \rightarrow \pi^+ l^+ l^-$	$-a_1 V_{ud} V_{cd}^*$	$M_1^{D^+}$	$\frac{1}{f_\pi}$
7	$D_s^+ \rightarrow K^+ l^+ l^-$	$a_1 V_{ud} V_{cd}^*$	$M_1^{D_s^+}$	$\frac{1}{f_K}$
8	$D^+ \rightarrow K^+ l^+ l^-$	$-a_1 V_{us} V_{cd}^*$	$M_1^{D^+}$	0
9	$D^0 \rightarrow K^0 l^+ l^-$	$-a_2 V_{us} V_{ud}^*$	$M_1^{D^0}$	0

weak annihilation contribution in Fig. 2(b) is determined by assuming that the vertices do not change significantly away from the kinematical region, where the heavy quark and chiral symmetries are good. We expect this to be a reasonable approximation in D meson decays. At the same time we use the full heavy meson propagators $1/(p_D^2 - m^2)$ instead of the heavy quark effective theory propagators $1/(2m v k)$ [31]. In the limit $m_P \ll m_D$, the bremsstrahlung-like diagrams in Fig. 2(b) cancel exactly, as explained in detail in the Secs. 3.3.3 and 5.5.1 of Ref. [32]. Only the non-bremsstrahlung weak annihilation diagrams in Fig. 2(a) render the nonvanishing contribution. The long distance amplitude is given by [32]

$$\begin{aligned} A^{LD}[D(p) \rightarrow P(p-q)l^+(p_+)l^-(p_-)] \\ = i \frac{G_F}{\sqrt{2}} e^2 A^{LD}(q^2) \bar{u}(p_-) \not{p} v(p_+), \end{aligned}$$

$$\begin{aligned} A^{LD}(q^2) = A_{peng.}^{LD}(q^2) + A_{bremsstrahlung}^{LD}{}_{annih.}(q^2) \\ + A_{non-brems.}^{LD}{}_{annih.}(q^2), \end{aligned} \quad (A5)$$

$$A_{peng.}^{LD}(q^2) = a_2 V_{cs}^* V_{us} \frac{1}{q^2} f_+(q^2) N_1(q^2),$$

$$A_{bremsstrahlung}^{LD}{}_{annih.}(q^2) \approx 0,$$

$$\begin{aligned} A_{non-brems.}^{LD}{}_{annih.}(q^2) = f_{Cabb}^{(i)} \frac{1}{q^2} M_1^{(i)}(q^2) f_P \left[-f_D \kappa \frac{m_P^2}{m_D^2 - m_P^2} \right. \\ \left. - \sqrt{m_D} \left(\alpha_1 - \frac{m_D^2 + m_P^2 - q^2}{2m_D^2} \alpha_2 \right) \right] \frac{\tilde{g}_V}{\sqrt{2}}, \end{aligned}$$

with Cabibbo factors $f_{Cabb}^{(i)}$ and the coefficients $M_1(q^2)$ and $K_{DP}^{(i)}$ as given in Table V. The coefficient N_1 is equal to

$$\begin{aligned} N_1(q^2) = \frac{g_\rho^2}{q^2 - m_\rho^2 + i\Gamma_\rho m_\rho} - \frac{g_\omega^2}{3(q^2 - m_\omega^2 + i\Gamma_\omega m_\omega)} \\ - \frac{2g_\phi^2}{3(q^2 - m_\phi^2 + i\Gamma_\phi m_\phi)} + \frac{g_\rho^2}{m_\rho^2} - \frac{g_\omega^2}{3m_\omega^2} - \frac{2g_\phi^2}{3m_\phi^2}, \end{aligned}$$

while the coefficients $M_1^{(i)}$ are given in terms of $M_1^{D^0}$, $M_1^{D_s^+}$, and $M_1^{D^+}$ in Table V:

$$\begin{aligned} M_1^{D^0} = \frac{g_\rho}{q^2 - m_\rho^2 + i\Gamma_\rho m_\rho} + \frac{g_\omega}{3(q^2 - m_\omega^2 + i\Gamma_\omega m_\omega)} + \frac{g_\rho}{m_\rho^2} \\ + \frac{g_\omega}{3m_\omega^2}, \\ M_1^{D_s^+} = -\frac{g_\rho}{q^2 - m_\rho^2 + i\Gamma_\rho m_\rho} + \frac{g_\omega}{3(q^2 - m_\omega^2 + i\Gamma_\omega m_\omega)} \\ - \frac{g_\rho}{m_\rho^2} + \frac{g_\omega}{3m_\omega^2}, \end{aligned} \quad (A6)$$

$$M_1^{D^+} = -\frac{2g_\phi}{3(q^2 - m_\phi^2 + i\Gamma_\phi m_\phi)} - \frac{2g_\phi}{3m_\phi^2}.$$

Note that $N_1(0) = M_1(0) = 0$ for $\Gamma(0) = 0$ and there is no pole arising from the photon propagator at $q^2 = 0$. The relative sign of the short and long distance penguin amplitudes agrees with Ref. [37], which is based on assumption of quark-hadron duality.

In order to account for the contributions of the excited vector mesons $\rho_{1,2}$, $\omega_{1,2}$, and $\phi_{1,2}$, as described in the main text, the coefficients N_1 and M_1 are replaced in the Eqs. (A5) and (A6) by

$$\begin{aligned}
N_1 \rightarrow N_1 &+ \sum_{k=1}^2 \frac{g_{\rho_k}^2}{q^2 - m_{\rho_k}^2 + i\Gamma_{\rho_k} m_{\rho_k}} - \frac{g_{\omega_k}^2}{3(q^2 - m_{\omega_k}^2 + i\Gamma_{\omega_k} m_{\omega_k})} \\
&- \frac{2g_{\phi_k}^2}{3(q^2 - m_{\phi_k}^2 + i\Gamma_{\phi_k} m_{\phi_k})} + \frac{g_{\rho_k}^2}{m_{\rho_k}^2} - \frac{g_{\omega_k}^2}{3m_{\omega_k}^2} - \frac{2g_{\phi_k}^2}{3m_{\phi_k}^2}, \\
M_1^{D^0} \rightarrow M_1^{D^0} &+ \sum_{k=1}^2 \frac{g_{\rho_k}}{q^2 - m_{\rho_k}^2 + i\Gamma_{\rho_k} m_{\rho_k}} \\
&+ \frac{g_{\omega_k}}{3(q^2 - m_{\omega_k}^2 + i\Gamma_{\omega_k} m_{\omega_k})} + \frac{g_{\rho_k}}{m_{\rho_k}^2} + \frac{g_{\omega_k}}{3m_{\omega_k}^2}, \quad (A7) \\
M_1^{D^+} \rightarrow M_1^{D^+} &- \sum_{k=1}^2 \frac{g_{\rho_k}}{q^2 - m_{\rho_k}^2 + i\Gamma_{\rho_k} m_{\rho_k}} \\
&+ \frac{g_{\omega_k}}{3(q^2 - m_{\omega_k}^2 + i\Gamma_{\omega_k} m_{\omega_k})} - \frac{g_{\rho_k}}{m_{\rho_k}^2} + \frac{g_{\omega_k}}{3m_{\omega_k}^2}, \\
M_1^{D_s^+} \rightarrow M_1^{D_s^+} &- \sum_{k=1}^2 \frac{2g_{\phi_k}}{3(q^2 - m_{\phi_k}^2 + i\Gamma_{\phi_k} m_{\phi_k})} - \frac{2g_{\phi_k}}{3m_{\phi_k}^2}.
\end{aligned}$$

-
- [1] G. Burdman, E. Golowich, J. Hewett, and S. Pakvasa, Phys. Rev. D **52**, 6383 (1995); A. Khodjamirian, G. Stoll, and D. Wyler, Phys. Lett. B **358**, 129 (1995); S. Fajfer, S. Prelovsek, and P. Singer, Eur. Phys. J. C **6**, 471 (1999); **6**, 751(E) (1999).
- [2] S. Fajfer, S. Prelovsek, and P. Singer, Phys. Rev. D **58**, 094038 (1998).
- [3] S. Fajfer, S. Prelovsek, and P. Singer, Phys. Rev. D **59**, 114003 (1999).
- [4] S. Fajfer, S. Prelovsek, P. Singer, and D. Wyler, Phys. Lett. B **487**, 81 (2000).
- [5] B. Bajc, S. Fajfer, and R.J. Oakes, Phys. Rev. D **54**, 5883 (1996); P. Singer, Acta Phys. Pol. B **30**, 3849 (1999); **30**, 3861 (1999).
- [6] S. Prelovsek and D. Wyler, Phys. Lett. B **500**, 304 (2001).
- [7] I. Bigi, G. Gabbiani, and A. Masiero, Z. Phys. C **48**, 633 (1990).
- [8] The D^0 - \bar{D}^0 mixing predictions were compiled in H. Nelson, hep-ex/9908021.
- [9] CLEO Collaboration, R. Godang *et al.*, Phys. Rev. Lett. **84**, 5038 (2000); FOCUS Collaboration, J.M. Link *et al.*, Phys. Lett. B **485**, 62 (2000).
- [10] E791 Collaboration, E.M. Aitala *et al.*, Phys. Rev. Lett. **86**, 3969 (2001); D. Sanders, Mod. Phys. Lett. A **15**, 1399 (2000); D.J. Summers, hep-ph/0011079; hep-ex/0010002; A.J. Schwartz, hep-ex/0101050.
- [11] E791 Collaboration, E.M. Aitala *et al.*, Phys. Lett. B **462**, 401 (1999); D.A. Sanders, hep-ex/0105028.
- [12] H. Park, talk "D mixing and rare decays" at International Conference on B physics and CP Violation, Taipei, Taiwan, 1999, hep-ex/0005044 (<http://www.phys.ntu.edu.tw/english/bcp3/>); D. Pedrini, talk at Kaon99, <http://sgimida.mi.infn.it/~pedrini/homepage.html>
- [13] Particle Data Group, D.E. Groom *et al.*, Eur. Phys. J. C **15**, 1 (2000).
- [14] M. Selen, Workshop on Prospects for CLEO/CESR with $3 < E_{cm} < 5$ GeV, Cornell University, 2001, <http://www.lns.cornell.edu/public/CLEO/CLEO-C/>; M. Selen (private communication).
- [15] P. Singer and D.-X. Zhang, Phys. Rev. D **55**, R1127 (1997).
- [16] E. Lunghi, A. Masiero, I. Scimemi, and L. Silvestrini, Nucl. Phys. **B568**, 120 (2000).
- [17] T. Inami and C.S. Lim, Prog. Theor. Phys. **65**, 297 (1981); A.J. Schwartz, Mod. Phys. Lett. A **8**, 967 (1993).
- [18] C. Greub, T. Hurth, M. Misiak, and D. Wyler, Phys. Lett. B **382**, 415 (1996).
- [19] G. Buchalla, A. Buras, and M.E. Leutenbacher, Rev. Mod. Phys. **68**, 1125 (1996).
- [20] M.J. Duncan, Nucl. Phys. **B211**, 285 (1983); J.F. Donoghue, H.P. Nilles, and D. Wyler, Phys. Lett. **128B**, 55 (1983).
- [21] M. Misiak, S. Pokorski, and J. Roseik, in *Heavy Flavours II*, edited by A. Buras and M. Lindner (World Scientific, Singapore, 1998), p. 795, hep-ph/9703442.
- [22] J.A. Casas and S. Dimopoulos, Phys. Lett. B **387**, 107 (1996).
- [23] F. Gabbiani, E. Gabrielli, A. Masiero, and L. Silvestrini, Nucl. Phys. **B477**, 321 (1996).
- [24] T.P. Cheng and M. Sher, Phys. Rev. D **35**, 3484 (1987); M. Sher and Y. Yuan, *ibid.* **44**, 1461 (1991).
- [25] G. Castro, R. Martinez, and J. Munoz, Phys. Rev. D **58**, 033003 (1998).
- [26] G. Ecker, A. Pich, and E. Rafael, Nucl. Phys. **B291**, 692 (1987).
- [27] M. Bauer, B. Stech, and M. Wirbel, Z. Phys. C **34**, 103 (1987); M. Neubert, V. Rieckert, B. Stech, and Q.P. Xu, in *Heavy Flavours*, edited by A.J. Buras and M. Linder (World Scientific, Singapore, 1992), p. 286.
- [28] M. Wise, Phys. Rev. D **45**, R2188 (1992); G. Burdman and J.F. Donoghue, Phys. Lett. B **280**, 287 (1992).
- [29] R. Casalbuoni *et al.*, Phys. Rep. **281**, 145 (1997).
- [30] M. Bando *et al.*, Phys. Rev. Lett. **54**, 1215 (1985); Nucl. Phys. **B259**, 493 (1985); Phys. Rep. **164**, 217 (1988).
- [31] B. Bajc, S. Fajfer, and R.J. Oakes, Phys. Rev. D **53**, 4957 (1996).
- [32] S. Prelovsek, Ph.D. thesis, Ljubljana University, hep-ph/0010106.
- [33] CLEO Collaboration, T.E. Coan *et al.*, hep-ex/0102007; CLEO

- Collaboration, M. Dubrovin, hep-ex/0105030.
- [34] S. Fajfer and P. Singer, Phys. Rev. D **56**, 4302 (1997).
- [35] A.B. Clegg and A. Donnachie, Z. Phys. C **62**, 455 (1994).
- [36] S. Godfrey and N. Isgur, Phys. Rev. D **32**, 189 (1985).
- [37] N. Paver and Riazuddin, Phys. Rev. D **45**, 978 (1992).
- [38] MILC Collaboration, C. Bernard *et al.*, Nucl. Phys. B (Proc. Suppl.) **83**, 289 (2000); A. Abada *et al.*, *ibid.* **83**, 268 (2000).
- [39] N. Isgur and M.B. Wise, Phys. Rev. D **42**, 2388 (1990).